Biochimica et Biophysica Acta 903 (1987) 142–154
Elsevier

BBA 73668

Melittin induces H_{II} phase formation in cardiolipin model membranes

A.M. Batenburg [a], J.C.L. Hibbeln [a], A.J. Verkleij [b] and B. de Kruijff [c]

[a] *Department of Biochemistry,* [b] *Department of Molecular Cell Biology and* [c] *Institute of Molecular Biology and Medical Biotechnology, State University of Utrecht, Utrecht (The Netherlands)*

(Received 6 March 1987)

Key words: Protein–lipid interaction; Melittin; Cardiolipin; Hexagonal H_{II} phase; Phosphatidylcholine; NMR, ^{31}P-; Freeze-fracture electron microscopy; Model membrane; (Bovine heart)

The interaction of melittin with bovine heart cardiolipin model membranes was investigated via binding assays, ^{31}P-NMR, freeze-fracture electron microscopy, small angle X-ray diffraction and fluorescence based fusion assays. A strong binding ($K_d < 10^{-7}$ M) appeared to be accompanied by the formation of large structures, resulting from a fusion process of extremely fast initial rate. As the melittin content is increased, bilayer structure is gradually lost and from a cardiolipin to melittin ratio of about 6 the lipid starts to organize itself in an hexagonal H_{II} phase. At lower temperatures ($T < 40\,^{\circ}C$) the coexistence of another structure is observed, characterized by a broad isotropic ^{31}P-NMR signal and giving rise to sharp X-ray reflections, most probably a cubic phase, as suggested also by freeze-fracture images, showing orderly stacked particles. The results are discussed in relation to contrasting observations on the structural changes induced by melittin in the zwitterionic phospholipid system of dipalmitoylphosphatidylcholine (Dufourcq, J. et al. (1986) Biochim. Biophys. Acta 859, 33–48). The biological relevance of the observations with respect to the process of protein insertion into membranes is indicated.

Introduction

Melittin, the main constituent of bee (*Apis mellifera*) venom, is a 26 amino acids long, highly basic and hydrophobic polypeptide. Since the hydrophilic and hydrophobic residues are unevenly distributed along its sequence, the charges mainly concentrated at the C-terminus, its structure is amphiphilic and makes it interact with detergents and natural and artifical pure lipid membranes [1–5]. Melittin influences the permeability properties of membranes [6–10] and affects the activity of membrane bound enzymes [11–13]. The nature of its interaction with phospholipid model membranes has been extensively investigated (for reviews, see Refs. 1, 5 and 14). Concerning changes in peptide structure upon lipid binding, optical rotary dispersion and circular dichroism measurements indicated a transition from an extended coil to about 70% α-helix [15–17], similar to its conformation in tetramers, which are formed at high concentration, high pH and high ionic strength [18]. Crystalline melittin is also organized as tetramers, in which the peptides form α-helical rods, nicked at position 11–12 [19].

Abbreviations: LUV, large unilamellar vesicles; *N*-NBD-PE, *N*-(7-nitrobenz-2-oxa-1,3-diazol-4-yl)phosphatidylethanolamine; *N*-Rh-PE, *N*-(lissamine rhodamine B sulfonyl)dioleoylphosphatidylethanolamine; NMR, nuclear magnetic resonance; PC, phosphatidylcholine; PE, phosphatidylethanolamine; PG, phosphatidylglycerol; SUV, small unilamellar vesicles.

Correspondence: A.M. Batenburg, Department of Biochemistry, State University of Utrecht, P.O. Box 80.054, 3508 TA Utrecht, The Netherlands.

With regard to the lipid component it was found that interaction was enhanced by the introduction of negatively charged phospholipids, leading to higher peptide-lipid stoichiometries and higher affinity constants [20]. Moreover, in binary mixtures of negative and zwitterionic lipids, melittin induced a shift of the gel to liquid-crystalline transition towards that of the zwitterionic lipid, suggestive of a phase separation into domains rich in negatively charged lipids binding melittin and peptide-poor domains mainly consisting of zwitterionic lipid [21]. Information about the influence of the peptide on the molecular properties of phosphatidylcholines has been derived from diphenylhexatriene fluorescence polarization measurements and Raman spectroscopy, which indicated a slight increase of order in the liquid-crystalline state and a decrease of order in the gel state [22–24]. Differential scanning calorimetry [24,25] showed little influence on the temperature of the phase transition in zwitterionic lipid systems and a melittin concentration dependent decrease of the transition enthalpy.

Recent studies of protein–lipid interaction (as reviewed in Ref. 26 and 36) have shown that certain peptides also can modulate the supramolecular organization of phospholipids, the data gathered so far suggesting that besides overall basicity or hydrophobicity, shape and amphiphilicity of the peptide determine its effect on lipid structure. As melittin combines all these features in a relatively small and well defined structure, it would be a well chosen model peptide to investigate this further. Moreover, knowledge of the influence of melittin on lipid organization is of special interest since its structure bears distinct resemblance [27,28] to the general structure of the signal peptides which have been proposed to be involved in the insertion into and passage through membranes of newly synthesized proteins [29–31]. Studies of the macroscopic organization of phospholipids interacting with melittin are of relatively recent date and have been limited until now to phosphatidylcholine systems. A fragmentation of the bilayers by the action of melittin was indicated by early observations on negative staining electron microscopy images [7], while other authors reported a clearance of the lipid suspensions upon addition of high concentrations of melittin [22,24]. Recently changes in the diameter of the lipid structures and the formation of nonspherical objects were observed [32,33]. Similar lipid-melittin complexes of discoidal shape were shown by others [34,35], using freeze-fracture electron microscopy, for dipalmitoyl-PC in the gel phase after incubation above the phase transition, whereas a closed vesicular structure was conserved above the melting temperature. At the highest melittin-lipid ratios these authors report the formation of still smaller particles, regardless of the physical state of the lipids, which ultimately show a hydrodynamic radius of about 50 Å and are interpreted as micelles.

In this study we report on changes in lipid organization induced by binding of melittin to cardiolipin, a negatively charged phospholipid and thus a preferred target of the peptide as stated before. The results obtained by combined ^{31}P-NMR, small angle X-ray diffraction and freeze-fracture electron microscopy investigations show that melittin induces dramatic structure changes in cardiolipin model membranes, at high melittin concentration leading to the formation of an H_{II} phase, a behaviour quite opposite to that of melittin interacting with phosphatidylcholines. These differences in morphology are correlated with a different depth of penetration of melittin into the lipid environment as reported in the accompanying article [37] and will be discussed there in relation to this insertion.

Materials and Methods

Materials

The sodium salt of bovine heart cardiolipin was either purchased from Avanti (Birmingham, AL), or purified according to [38]. *N*-Rh-PE and *N*-NBD-PE were from Avanti; egg PC was purified from hen eggs using standard procedures. The purity of the lipids was confirmed by thin-layer chromatography. Melittin from commercial sources was found to contain considerable phospholipase contamination (see the accompanying article [37]). Phospholipase free melittin was obtained either by butanol extraction [39] both from whole venom and from commercially available melittin samples obtained from Serva or Sigma, or by applying the covalent chromatography based

purification method outlined in the accompanying article. After all experiments the absence of any phospholipid degradation products was checked and confirmed by thin-layer chromatography. All other chemicals were of analytical grade or better.

Model membranes

Unsonicated lipid dispersions were formed by hydration of a dry lipid film in buffer. Small unilamellar vesicles (SUV) were obtained from lipid dispersions by a 50 W, 10×30 s sonication under nitrogen with a 0.5 inch flat disruptor tip mounted on a Branson B12 sonifier, while cooling with ice-water. SUV were isolated as the supernatant of a 10 min $27\,000 \times g$ centrifugation. Large unilamellar vesicles (LUV) were prepared by the slightly modified [40] reversed phase evaporation technique [41]: 1 ml diethyl ether, containing 7.5 mg of lipid, is sonicated with 3 ml of buffer in a bath-sonicator to form an emulsion, followed by a controlled removal of the ether. The vesicles thus obtained were 'sized' by extrusion through a 0.2 μm Unipore polycarbonate membrane. All types of vesicles and melittin stocks were prepared and all experiments performed in a buffer containing 100 mM NaCl, 10 mM Tris, 1 mM EDTA (pH 7.0) at a temperature of 25°C, unless otherwise stated. Phospholipid was determined as inorganic phosphate after destruction with perchloric acid [42,43].

Binding assay

Peptide-lipid binding experiments were performed by addition of different amounts of a melittin solution to 20 nmol cardiolipin (unsonicated dispersions) in a total volume of 200 μl. After a 30 min incubation at 37°C and a 20 min $27\,000 \times g$ centrifugation at 4°C in a Sorvall RCB2 the amount of unbound peptide was determined by measurement of the fluorescence of the 20-fold diluted supernatant with an Perkin-Elmer MPF3 fluorometer, the excitation and emission wavelengths set at 280 and 350 nm. No lipid was detectable in the supernatant; applying the procedure to melittin without lipid resulted in a complete recovery of the peptide and incubation and centrifugation of lipid in the absence of melittin did not lead to higher values of fluorescence than blancs of buffer only. The binding data were analysed by means of an iterative non-linear regression computer program, developed to calculate the amount of lipid monomers constituting one peptide binding site N, and the dissociation constant K_d, defined by the equation $K_d = [P] \cdot [L_N]/[PL_N]$ in which [P] and $[L_N]$ represent the concentrations of free peptide and free peptide binding sites, respectively, the last variable by definition being the concentration of free lipid divided by the amount of lipids per binding site [44].

^{31}P-NMR

^{31}P-NMR measurements were carried out either at 81.0 MHz with a Bruker WP 200 or at 121.5 MHz with a Bruker MSL 300, while applying broadband decoupling as described before [45]. Typically 20000 45° pulses with an interpulse time of 1 s were employed on 1 ml unsonicated dispersions containing 10 μmol cardiolipin, to which melittin was added as a 50 mM solution. To suppress the noise an exponential filtering of the free induction decays was applied resulting in a line broadening of 50 Hz for 81.0 MHz and of 75 Hz for 121.5 MHz spectra, respectively.

Small-angle X-ray scattering

For X-ray diffraction measurements various amounts of a 2 mM melittin solution were added to cardiolipin unsonicated dispersions (1 μmol cardiolipin) to make a total volume of 1 ml. The samples were concentrated by centrifugation and the pellets were transferred into the $0.5 \times 1.5 \times 16$ mm slits of the sample holders, which were closed with cellophane. The samples were irradiated for 30 min with a 1×0.2 mm copper K_α beam (40 kV, 20 mA) in a Kratky camera equipped with a position sensitive LETI detector, interfaced to a microcomputer.

Freeze-fracture electron microscopy

SUV containing 1 μmol of cardiolipin were mixed with a 2 mM melittin solution in a total volume of 1 ml. After pelleting the melittin-cardiolipin complexes, they were quenched by plunge freezing with the Reichert Jung KF 80 [46] without the use of cryoprotectants. The freeze-fracture replicas were analysed with a Philips 420 microscope.

Fusion assays

LUV fusion induced by melittin was followed with two fluorescence based methods. Mixing of aqueous vesicle contents was monitored with an assay developed by Wilschut et al. [40]. The other method [47] is designed to examine the mixing of vesicle lipids. The dilution of the fluorescent probes *N*-Rh-PE and *N*-NBD-PE, originally contained in one vesicle population (3 mol% P_i each), by fusion with a 19-fold excess of unlabelled vesicles is reflected as a decrease of efficiency of resonance energy transfer between the probes, measured as an increase of NBD fluorescence at 530 nm. A 100% fusion value was established by measurement of the fluorescence of a third LUV population containing 0.15% of both probes, to which a saturating amount of melittin was added in order to obtain lipid-peptide complexes of comparable structure. Blancs, obtained by measuring the effect of melittin addition to a nonfluorescent vesicle population, were always subtracted to correct for increase in light scattering induced by melittin. The experiments were performed with a Perkin-Elmer MPF3 fluorometer.

Results

Binding experiments

Binding experiments were performed in order to obtain insight into the stoichiometry of the cardiolipin-melittin complex and its strength of association. Addition of melittin to cardiolipin dispersions caused an immediate increase of turbidity and at high peptide-cardiolipin molar ratios ($> 1/5$) a visual precipitation of the phospholipid. This process appears to be the result of a high-affinity binding of the melittin to the lipid (Fig. 1). From the data of the binding experiments a stoichiometric ratio of one melittin bound per 1.98 ± 0.08 cardiolipin molecules was calculated. If the double charge of the cardiolipin molecule is taken into consideration, this value is in good agreement with earlier data [20] which showed a stoichiometry of one melittin bound to three or four negative charges in the melittin-phosphatidylserine complex. Exactly the same ratio was found in complementary experiments in which the melittin was not added to preformed dispersions, but instead was present in the buffer used to disperse the dry lipid film. These studies show that binding of melittin is not restricted to the outer monolayers of the vesicles but rather that melittin causes a change in lipid organization by which it can gain access to additional binding sites. The dissociation constant could not be determined accurately from these binding data, but certainly was smaller than 10^{-7} M.

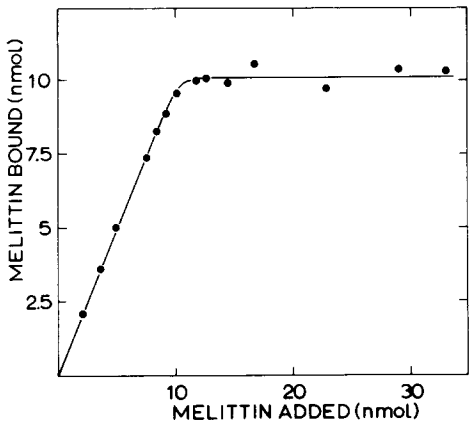

Fig. 1. Binding of melittin to unsonicated dispersions of bovine heart cardiolipin. The amount of cardiolipin was held constant at 20 nmol. Experimental detail is presented under Materials and Methods.

^{31}P-NMR

^{31}P-NMR is a covenient tool to study lipid polymorphism [26,36]. The shape of the spectrum provides a reliable [48] criterion to discriminate between different phospholipid structures. The 81 MHz ^{31}P-NMR-spectrum of pure cardiolipin (Fig. 2a) shows the high-field peak and low-field shoulder of a signal resulting from partial averaging of chemical shift anisotropy by fast axial motion of the phosphates in a random collection of extended bilayers [49] which henceforth will be referred to as 'bilayer spectrum'. The small amount of signal around the chemical shift position of phospholipid experiencing isotropic motion almost certainly originates from cardiolipin organized in small vesicles and appears to be customary to cardiolipin dispersions [50,51]. Upon addition of increasing amounts of melittin (Figs. 2b–2e) the contribution of the isotropic signal to the spectrum gradually increased and at the saturating melittin to cardiolipin ratio of 1 : 2.0 (Fig. 2e) no 'bilayer spectrum' was observed any-

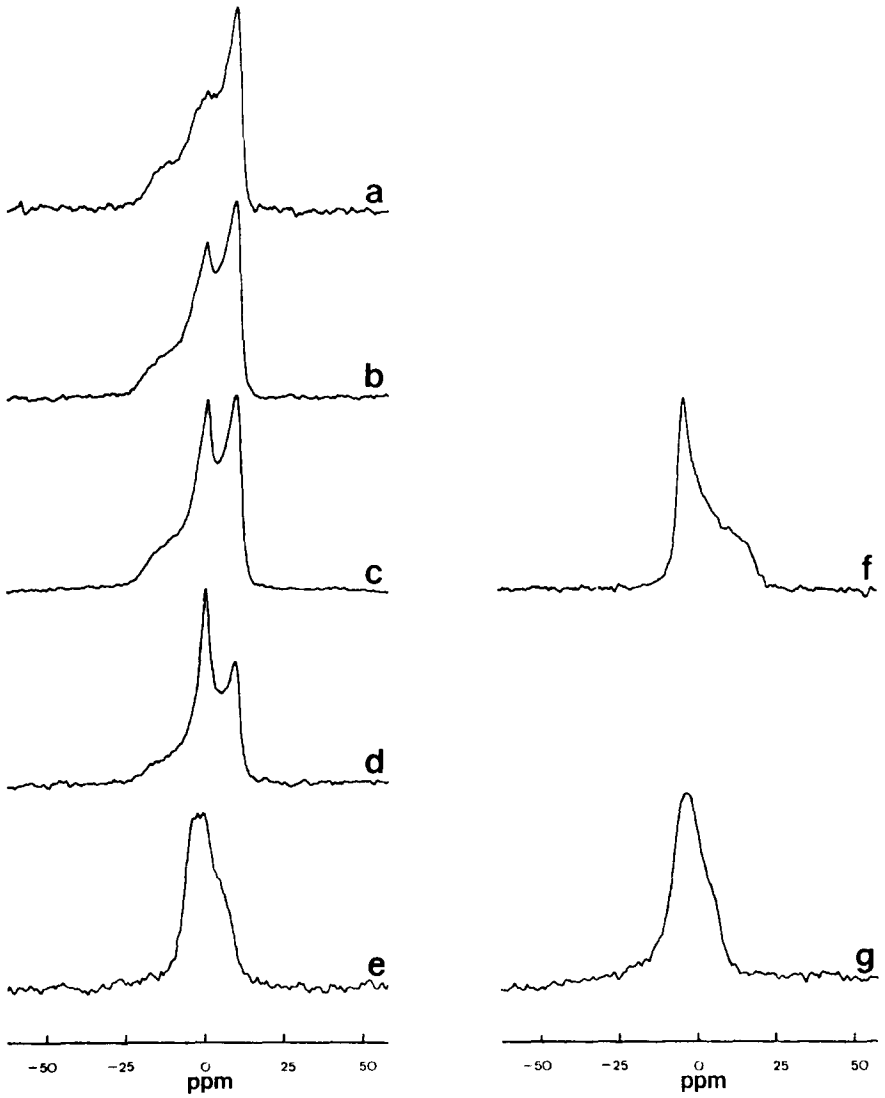

Fig. 2. 81.0 MHz ^{31}P-NMR spectra of cardiolipin dispersions before (a) and after addition of increasing amounts of melittin (b–g). Melittin to cardiolipin molar ratio: 1 : 30 (b); 1 : 15 (c); 1 : 6 (d) and 1 : 2.0 (e). f and g: spectra recorded after addition of an excess Ca^{2+} (2 moles of Ca^{2+} per mol cardiolipin) to the samples containing melittin-cardiolipin complexes of 1 : 15 and 1 : 2.0 molar ratio, respectively. The chemical shift position of the signal of sonicated egg PC vesicles is at 0 ppm.

more. The decrease of this 'bilayer' contribution to the spectrum is directly proportional to the amount of melittin added (Fig. 3); as the data points were chosen to cover a wide range of peptide-lipid ratios, this is most clearly shown using double logarithmic axes. Although at this stage the origin of the lipid structure giving rise to the isotropic component is unclear, the linear relationship of its appearance with increase in melittin concentration implicates that this structure is already formed at low melittin-lipid ratios and that the complex has a well defined stoichiometry of 1 : 2.0 (Fig. 3) matching that of the binding. Unfortunately ^{31}P-NMR is not capable of discerning the different structures that allow isotropic motion of the phospholipids (small vesicles, micelles, small bilayer discs, inverted micelles, cubic phases). The first three possibilities however are highly improb-

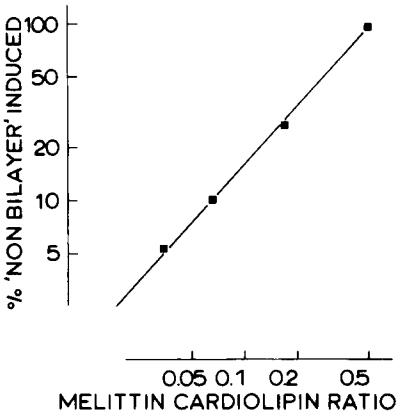

Fig. 3. Change of the ^{31}P-NMR spectrum of cardiolipin dispersions as a function of the amount of melittin added. For the calculation of this plot with double natural logarithmic scale the fraction corresponding to the isotropic signal of the pure cardiolipin spectrum was left out of consideration. For spectra composed of 'bilayer' and isotropic signal, intensities were calculated by subtracting the underlying bilayer spectrum that was estimated from Fig. 2a.

able on account of the fact that a short centrifugation step leads to a complete pelleting of the phospholipid.

Addition of a 2-fold excess of calcium to the melittin-cardiolipin 1:15 complex resulted in a complete transition to an H_{II} phase, with a phosphate chemical shift anisotropy similar to that of a pure Ca^{2+}-cardiolipin H_{II} phase, indicating that melittin does not stabilize the bilayer organization. In the melittin-saturated complex no major influence of Ca^{2+} is observed (compare Figs. 2e and 2g).

Since the lineshape of the ^{31}P-NMR spectrum of the saturated melittin-cardiolipin complex (Fig. 2e) is of insufficient quality to allow an unambiguous interpretation, attempts were made to improve it. Mixing the two components in a larger volume (1 mM cardiolipin) to improve sample homogeneity, and recording the spectrum at higher magnetic fieldstrength, which in general leads to better defined lineshapes, resulted in the NMR spectrum of Fig. 4a. From this much easier interpretable spectrum, which shows only a minor isotropic component superimposed on a signal typical for phospholipids undergoing fast lateral diffusion around cylindrical structures such as found in the H_{II} phase, a residual ^{31}P-chemical shift anisotropy of 14 ppm was determined, which matches exactly

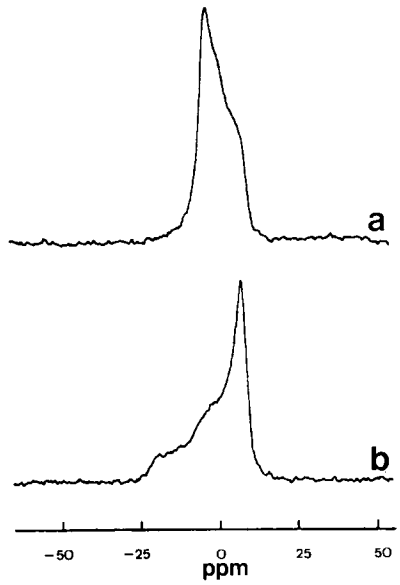

Fig. 4. 121.5 MHz ^{31}P-NMR spectra of cardiolipin dispersions before (b) and after (a) addition of a saturating amount (1:2.0 mol/mol) of melittin. 0 ppm corresponds to the chemical shift position of the signal of lysophosphatidylcholine micelles.

half the 28 ppm large ^{31}P-chemical shift anisotropy of the phosphates of the pure cardiolipin bilayer (Fig. 4b). Such a reduction of the chemical shift anisotropy by a factor of two can be theoretically inferred [53] for a transition from bilayer to hexagonal phase, assuming that no change in local order of the phosphate group occurs. It is worth noting that the observed chemical shift anisotropy is considerably smaller than the 21 ppm chemical shift anisotropy of the calcium induced H_{II} phase of cardiolipin (Ref. 52 or Fig. 2f). No time dependency of the ^{31}P-NMR spectra was observed.

Freeze-fracture electron microscopy

For electronmicroscopy experiments SUV were taken as starting material to get a good sample homogeneity and to visualize possible fusion phenomena; from a melittin to cardiolipin ratio of 1:20 onwards very similar results were obtained using unsonicated dispersions. After freeze-fracturing, the SUV appeared as small (300 Å diameter) highly curved bilayer structures (data not shown) and in agreement with the ^{31}P-NMR results, addition of melittin to cardiolipin vesicles resulted in marked changes in freeze-fracture morphology. At low melittin-phospholipid ratios (Figs.

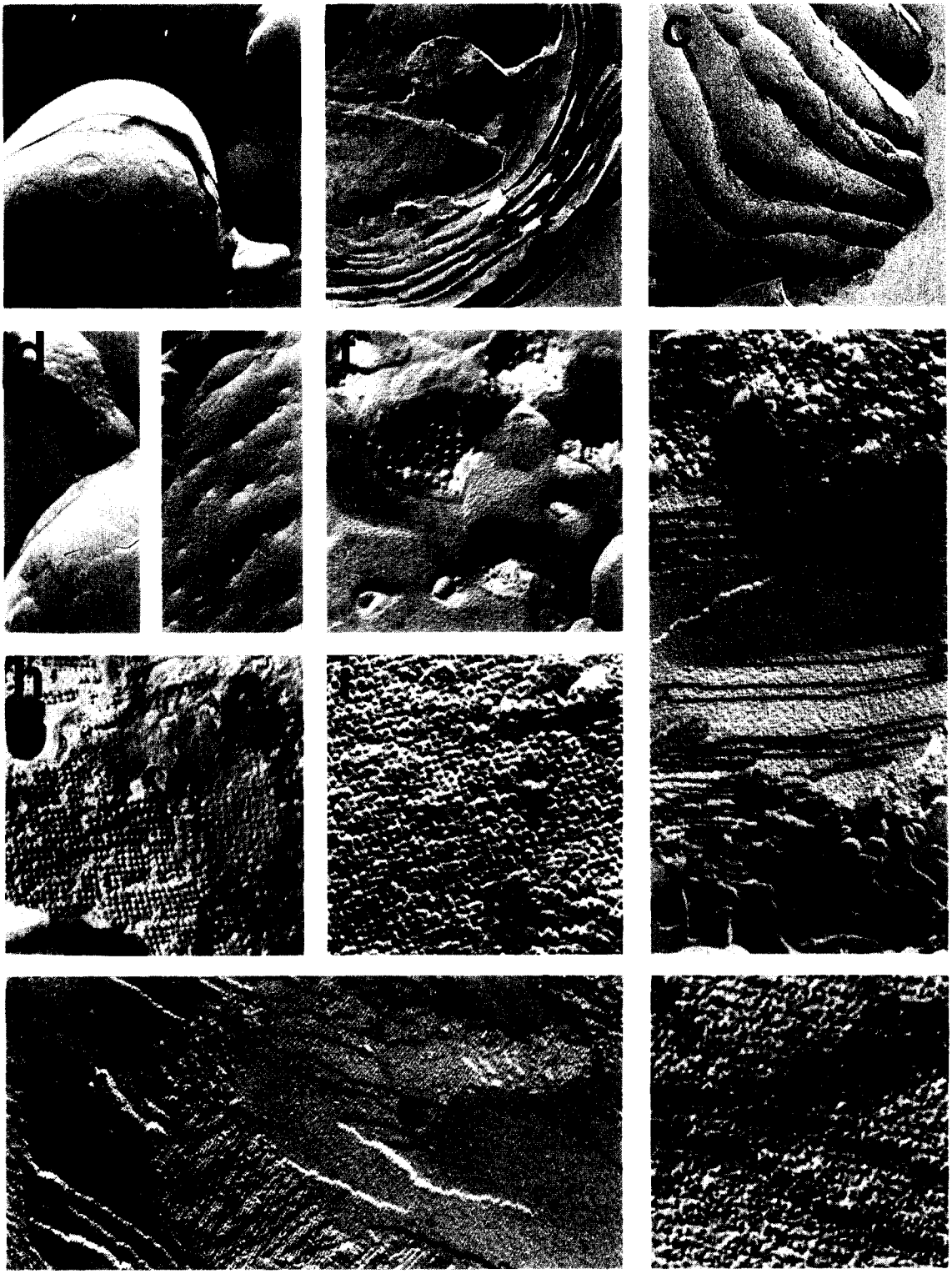

Fig. 5. Freeze-fracture morphology of the cardiolipin-melittin complexes. Melittin was added to cardiolipin SUV in a molar ratio of 1:15 (a–e); 1:10 (f); 1:5 (g–i) and 1:1.8 (j and k). Magnification: 55000× (a, b and d), 72000× (c, e, g, h and j), 88000× (f and i) and 300000× (k).

5a–5f), mostly smooth extended bilayers are visualized usually stacked in multilayered structures as shown by Fig. 5a and, in cross-section, in Fig. 5b. The existence of extended bilayer sheets points to a thorough reorganization of the phospholipids, since small single-walled vesicles were taken as starting material. Fig. 5c shows ridges and complementary fissures, similar to those seen in Fig. 4c of Ref. 60, that were interpreted to reflect inverted tubular structures. In the same reference the ill-defined pits observed at this melittin-lipid ratio (Fig. 5e) were suggested to represent the 'adhesion' sites in the first stage of a fusion event. More abundant are the patches of spherical particles of well-defined shape (Fig. 5f); the presence of complementary pits (Fig. 5d) has earlier been taken as evidence for a lipidic nature of the particles. At higher melittin concentrations (Figs. 5g–5i), the particles are no longer randomly scattered and the replicas instead show the appearance of well ordered cubic arrays with a particle diameter of about 140 Å. Most often the array visualized is restricted to two dimensions, at some places, however, (Fig. 5h) a three-dimensional ordering can be observed. Complementary fracture faces with regularly spaced pits (Fig. 5h) could represent layers bounding cubicly stacked regions. Besides cubic arrays some bilayer remnants and some striated patterns typical of the hexagonal H_{II} phase are visualized at this 1 : 5 molar ratio (Fig. 5g). H_{II} phase is dominating in cardiolipin samples saturated with melittin (Figs. 5j and 5k), for which a tube diameter of approx. 67 Å was determined.

Small angle X-ray diffraction

X-ray irradiation of pure cardiolipin unsonicated dispersions results in a very weak scattering, while sharp reflections are totally absent (Fig. 6a), indicating either (1) an irregular or very large spacing between lamellae of multilayered vesicles, or (2) the predominance of unilamellar structures in these dispersions as suggested by others [54]. From a melittin-cardiolipin ratio of 1 : 12 onwards, addition of melittin results in the appearance of a scatter-maximum centered around 40–50 Å (Fig. 6, b and c) without discrete diffraction lines, thus not showing the regular stacking of bilayers, that was seen in the cardiotoxin II-

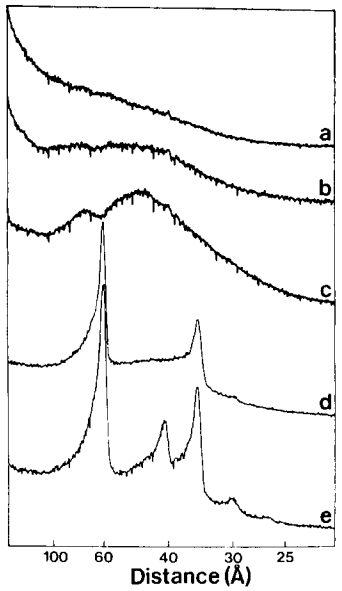

Fig. 6. Small angle X-ray scattering patterns of melittin-cardiolipin systems. Melittin was added to cardiolipin MLV in a molar ratio of 1 : 15 (b); 1 : 6 (c) and 1 : 1.8 (d and e). Profile (a) represents the scattering of cardiolipin unsonicated dispersions without melittin.

cardiolipin [50] or more clearly in the polylysine-cardiolipin system [55]. From a melittin-cardiolipin ratio of 1 : 6 onwards however, sharp reflections do arise, which persist till saturation with melittin (Figs. 6, d and e). In very rare cases, under these circumstances, a relatively simple pattern is observed with spacings of $1 : 1/\sqrt{3} : 1/2$ that can be expected to result from the hexagonal stacking of tubes in a pure H_{II} phase. In the vast majority of the samples ($n = 30$), however, additional peaks were observed (Fig. 6 e), corresponding to repeat distances of about 41 and 27 Å, not related to other reflections by any simple spacing ratio. It is tempting of course to correlate the appearance of these peaks with the cubic arrays of particles observed with freeze-fracture of similar samples. A cubic lipid phase that seems to fit our data has indeed been described [56]. Our reflections could represent the $1/\sqrt{3}$ and $1/\sqrt{7}$ peaks, respectively, of this Q230 lattice, described to consist of two intertwined but unconnected tubular networks [56] for which spacings of $1/\sqrt{3} : 1/2 : 1/\sqrt{7} : \ldots$ were reported; the 1/2 reflection would then be masked by the nearby $1/\sqrt{3}$ peak of the dominating H_{II} phase pattern. The fit

of this analysis of the small angle X-ray scattering pattern with the experimental data is demonstrated in Table I. This table furthermore indicates a tube diameter of the H_{II} phase of 68 ± 1 Å, which is calculated as $2/\sqrt{3}$ times the first order reflection and which is in good accordance with the electronmicroscopic data. This value is about 4 Å larger than that of the Ca^{2+} induced H_{II} phase of cardiolipin. From a melittin to cardiolipin ratio of 1 : 10, experiments with SUV instead of unsonicated dispersions produced very similar diffraction profiles.

Temperature dependence

Whereas time appeared not to influence significantly the relative abundance of the two lattices in a sample as judged from the intensities of their small angle X-ray reflections, temperature was found to have a marked effect on the equilibrium as demonstrated by Fig. 7. Quantitative information from ^{31}P-NMR (Fig. 8) indicates that the disappearance of the reflections of the 'cubic' lattice at higher temperatures correlates with a phase transition. At low temperatures the spectrum is dominated by a broad isotropic type of signal which can well reflect lipids in a cubic phase, and shows a gradual transition to a typical H_{II} signal as the temperature is raised. The circumstances under which no isotropic contribution was observed, correlated well with the conditions necessary to obtain a pure H_{II} diffraction pattern.

The temperature dependence of the small angle X-ray scattering profile also provides additional evidence for the relationship between the 41 and 27 Å reflections, as they are shown to disappear together upon raising the temperature. The reflections of both lattices show a significant and reversible decrease of unit dimensions at higher temperatures.

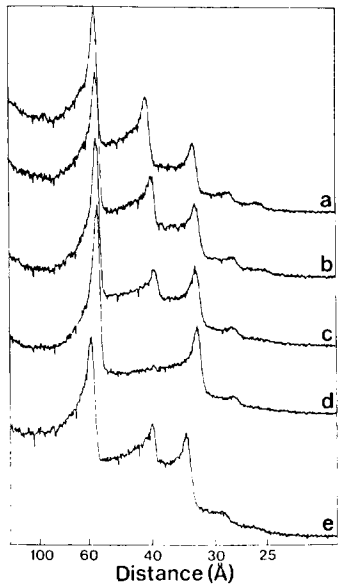

Fig. 7. Small angle X-ray diffraction of a melittin-cardiolipin sample of molar ratio 1 : 2.0 at 5 °C (a); 20 °C (b); 30 °C (c) and 45 °C (d) and at 20 °C after heating to 45 °C (e).

Fusion experiments

Freeze-fracturing of cardiolipin SUV to which melittin was added in a relatively low peptide-lipid ratio indicated a drastic reorganization of the lipid, resulting in extended bilayer sheets. This change in morphology can only be brough about by some

TABLE I

SMALL ANGLE X-RAY DIFFRACTION DATA ON MELITTIN-CARDIOLIPIN (1 : 2.0 mol/mol) COMPLEXES AND THE RELATED Ca^{2+}-CARDIOLIPIN SYSTEM

Samples were prepared as described under Materials and Methods. The values between [] indicate the relationship between the first and higher order reflections, whereas values between () refer to the expected spacings calculated from the lowest order reflection observed using this relationship.

	d value (Å)				
Melittin/cardiolipin (1 : 2.0), experimental	59.2	40.5	34.5	29.4	26.4
Hexagonal lattice	[1]		[$1/\sqrt{3}$](34.2)	[1/2](29.6)	
Cubic lattice [a]		[$1/\sqrt{3}$]	[1/2](35.0)		[$1/\sqrt{7}$](26.5)
Ca^{2+}/cardiolipin (1 : 1), experimental [b]	55.8[1]		32.4[$1/\sqrt{3}$]	27[1/2]	

[a] As described by Luzzati et al. [56].
[b] According to De Kruijff et al. [55].

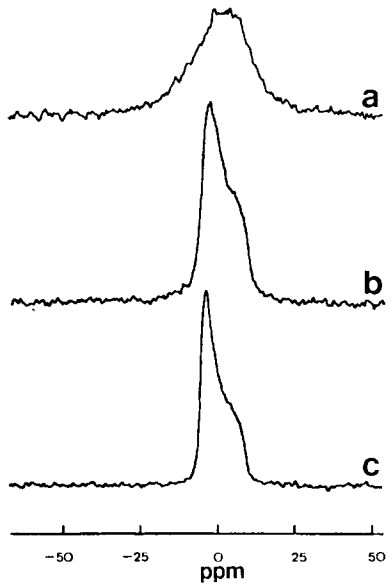

Fig. 8. 121.5 MHz ^{31}P-NMR spectra of cardiolipin dispersions to which melittin was added in a ratio of 1:1.5 at 5 °C (a) and after heating to 30 °C (b) and 45 °C (c). 0 ppm represents the signal position of lysophosphatidylcholine micelles.

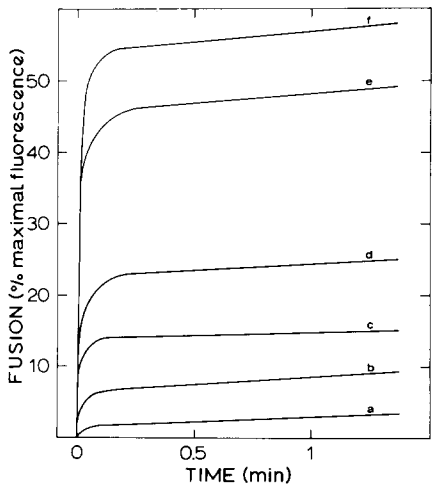

Fig. 9. Melittin-induced fusion of cardiolipin LUV, observed with the lipid mixing assay. Melittin was added as a 250 μM solution to 25 μM cardiolipin in a final volume of 2 ml. Melittin to cardiolipin molar ratio: 1:60 (a); 1:25 (b); 1:12 (c); 1:7 (d); 1:4.3 (e) and 1:1.7 (f). An excitation wavelength of 450 nm and an emission wavelength of 530 nm were used.

kind of a fusion process. The character and kinetics of this fusion were investigated by assays monitoring either the mixing of the lipids [47] or of the aqueous contents [40] of two different LUV populations.

The lipid mixing assay showed initially a very rapid 'burst' of fusion, followed by a much slower fusion phase (Fig. 9). A complete mixing of vesicles was not achieved during the time course studied; in case of a high melittin-lipid ratio the measurements could not be prolonged due to an excessive turbidity increase and precipitation of the lipid material. Experiments with SUV instead of LUV also resulted in a fusion of extremely fast initial rate (data not shown).

With the assay based on mixing of vesicle contents [40], measuring the formation of the fluorescent terbium-dipicolinate complex, it is possible to discriminate fusion processes during which the barrier properties of the vesicles remain intact, from those accompanied by leaks leading to a dissociation of the fluorophore by EDTA outside the vesicles. Application of this technique to melittin induced fusion of cardiolipin LUV, under the same conditions as used for the lipid mixing assay, did not result in the formation of the fluorescent complex, in contrast to the Ca^{2+} triggered fusion of cardiolipin-PC mixed vesicles [57] and of pure cardiolipin vesicles (unpublished observations). This suggests a leaky kind of fusion as was indeed evidenced by performing this assay in the absence of external EDTA, which did show the appearance of the terbium-dipicolinate complex on a time scale comparable to that of lipid mixing, thus indicating a loss of barrier function which allows the passage of relatively large solutes. Attempts to seal the vesicles during fusion by making use of mixed lipid vesicles containing 80% PC and 20% cardiolipin (P_i based) were not successful. Taken together with results of others, who observed non-leaky fusion using LUV of a mixture of PE, PC and cardiolipin [58], this indicates that a more balanced lipid composition is obligatory for retainance of contents.

Discussion

The most important observation in this study was the induction of a hexagonal H_{II} phase by the action of melittin on cardiolipin model membranes. We will discuss two aspects of this phenomenon, namely its mechanism and its lipid specificity.

The binding experiments indicate a strong ($K_d < 10^{-7}$ M) interaction of melittin with cardiolipin model membranes with a stoichiometry of one melittin monomer bound per two molecules of cardiolipin. Assuming the +6 charge of the melittin molecule to be preserved upon binding, this ratio obviously does not lead to complete charge compensation. In accordance with earlier reports [10,58] melittin was found to induce vesicle fusion, resulting in a change in morphology from small unilamellar vesicles to large, often stacked sheets of bilayer structure. Also suggestive of fusion events are the ridges and fissures, while the particles observed by electron microscopy in these samples could possibly play a role in the fusion process if assumed to represent point-fusion intermediates as suggested before [53]. The biphasic kinetics of the fusion process as observed with the lipid-mixing assay may be related to high local concentrations of melittin, initially affecting only that part of the vesicles to which it is bound.

This fusion process leads to the formation of large complexes containing highly curved lipid structures as indicated by the appearance of an isotropic ^{31}P-NMR signal, which is correlated with the presence of particles on the fused bilayers visualized by electron microscopy, possibly representing inverted lipidic structures as suggested by the complementary pits. This idea is reinforced by the observation that at higher melittin content the lipid organizes in the inverted tubular structures of an H_{II} phase [59].

At low temperatures in the final situation however next to the H_{II} phase, a different phase was observed with NMR and small angle X-ray scattering, giving rise to sharp X-ray reflections, which was correlated with the appearance of large, well defined, orderly stacked particles, visualized by freeze-fracturing. Similar electron microscopic images in situations intermediate between bilayer and H_{II} phase in PE/PC mixtures [60] and in cardiolipin containing systems [61] have been suggested to reflect closely packed inverted micelles; on the basis of X-ray diffraction studies however, others [56,62] have argued that these pseudo-crystalline structures in fact represent interwoven networks of branched rods which may be of either type I or II with the polar phase facing outside or inside, respectively, a view supported also by recent evidence [63]. A type II structure obviously is more likely in the melittin-cardiolipin complex in view of its relationship with the inverted H_{II} phase which is favoured at high temperatures. Although the abundance of this cubic array in the melittin-cardiolipin 1 : 5 complex suggests this phase also to be a ratio dependent intermediate structure between lamellar and H_{II} phase, no samples could be obtained which showed X-ray reflections of this structure only. This sample heterogeneity as well as the small amount of reflections observed do not allow an unequivocal phase identification.

The formation of large structures, at high melittin content resulting in inverted tubular organizations, indicates a marked difference with the structural reorganizations induced by melittin in the dipalmitoyl-PC system [34,35,64]. In this zwitterionic lipid system at high melittin concentration very small structures have been reported, interpreted as micelles [35]. According to the shape-structure concept of lipid polymorphism [65], micelles or in general type I structures with polar groups facing outside, are formed when the space occupied in the headgroup region by the molecules exceeds that in the apolar region, while the opposite situation leads to type II (inverted) structures; bilayer organization then is a result of the intermediate case, when the bulkiness of the molecules is not explicitly depth-dependent. From this point of view the influence of melittin on supramolecular organization in the two compared systems is completely opposite and cannot be explained by the assumption of a simple wedge-like behaviour of melittin functioning as a headgroup spacer as proposed before [8]. The differences between the two lipid systems may be related to a different positioning of the melittin with respect to the surrounding lipid in terms of orientation or depth of penetration. This suggestion is addressed with fluorescence quenching techniques in the accompanying article [37], where also a rationale for the lipid specificity is developed.

Another point of interest is the lipid specificity of the observed phenomena with regard to other negatively charged phospholipids. Very recent ^{31}P-NMR experiments with ditetradecyl-PG [67] showed at high melittin-lipid ratio the appearance of an isotropic signal. On basis of this observation alone, however, no structural assignment can be

made, since very different structures can give rise to such type of signal, as stated above. Further studies with other techniques will be necessary to see if the melittin-induced changes in macroscopic organization of bovine heart cardiolipin can be extrapolated to other negatively charged phospholipids, which, as emphasized before, form a preferred binding site for melittin.

Finally with respect to the biological relevance of the observations, it can be claimed that in principle amphipathic peptides indeed are capable to effect a transition from a bilayer to an inverted lipid structure. Although high peptide concentrations are necessary to visualize these changes by physical techniques, extrapolation of the results (see Fig. 3 and its discussion) suggests local deviations from the bilayer structure to occur already at low peptide to lipid ratios. Similar local changes, which could be brought about by the action of the structurally much related signal peptides, which have recently been shown to interact with phospholipids [66,67], may be of importance for the process of protein translocation across membranes.

Acknowledgements

We would like to thank J. Leunissen-Bijvelt for performing the freeze-fracture experiments. This study was carried out under the auspices of the Netherlands Foundation for Chemical Research (S.O.N.) and with financial aid from the Netherlands Organization for the advancement of Pure Research (Z.W.O.).

References

1 Habermann, E. (1972) Science 177, 314–322
2 Mollay, C. and Kreil, G. (1973) Biochim. Biophys. Acta 316, 196–203
3 Bhakoo, M., Birckbeck, T.H. and Freer, J.H. (1982) Biochemistry 21, 6879–6883
4 Läuterwein, J., Bösch, C., Brown, L.R. and Wüthrich, K. (1979) Biochim. Biophys. Acta 556, 244–264
5 Dufourcq, J., Dasseux, J.L. and Faucon, J.-F. (1984) Bacterial Protein Toxins 24, 127–138
6 Habermann, E. and Kowallek, H. (1970) Hoppe-Seyler's Z. Physiol. Chem. 351, 884
7 Sessa, G., Freer, J.H., Colaccico, G. and Weissman, G. (1969) J. Biol. Chem. 244, 3575–3582
8 Yianni, Y.P., Fitton, J.E. and Morgan, C.G. (1986) Biochim. Biophys. Acta 856, 91–100
9 Tosteson, M.T. and Tosteson, D.C. (1981) Biophys. J. 36, 109–116
10 Morgan, C.G., Williamson, H., Fuller, S. and Hudson, B. (1983) Biochim. Biophys. Acta 732, 668–674
11 Boone, L.R. and Skalka, A. (1980) Proc. Natl. Acad. Sci. USA 77, 847–851
12 Vesely, D.L. (1981) Science 213, 359–360
13 Pellkofer, R., Marsh, D., Hoffmann-Bleihauser, P. and Sandhoff, K. (1982) J. Neurochem. 38, 1230–1235
14 Habermann, E. (1980) in 'Natural Toxins' (Eaker, D. and Wadström, T., eds.), pp. 173–181, Pergamon Press, New York
15 Talbot, J.C., Dufourcq, J., De Boni, J., Faucon, J.-F. and Lussan, C. (1979) FEBS Lett. 102, 191–193
16 Vogel, H. (1981) FEBS Lett. 134, 37–42
17 Drake, A.F. and Hider, R.C. (1979) Biochim. Biophys. Acta 555, 371–373
18 Bello, J., Bello, H.R. and Granados, E. (1982) Biochemistry 21, 461–465
19 Terwillinger, T.C. and Eisenberg, D. (1982) J. Biol. Chem. 257, 6016–6022
20 Dufourcq, J. and Faucon, J.-F. (1977) Biochim. Biophys. Acta 467, 1–11
21 Bernard, E., Faucon, J.-F. and Dufourcq, J. (1982) Biochim. Biophys. Acta 688, 152–162
22 Lavialle, F., Levin, I. and Mollay, C. (1980) Biochim. Biophys. Acta 600, 62–71
23 Jähnig, F., Vogel, H. and Best, B. (1982) Biochemistry 21, 6790–6798
24 Dasseux, J.L., Faucon, J.F., Lafleur, M., Pézolet, M. and Dufourcq, J. (1984) Biochim. Biophys. Acta 775, 37–50
25 Mollay, C. (1976) FEBS Lett. 64, 65–68
26 De Kruijff, B., Cullis, P.R., Verkleij, A.J., Hope, M.J., Van Echteld, C.J.A., Taraschi, T.F., Van Hoogevest, P., Killian, J.A., Rietveld, A. and Van der Steen, A.T.M. (1985) in 'Progress in Protein-Lipid Interactions' (Watts, A. and De Pont, J.J.H.H.M., eds.), pp. 89–142, Elsevier Biomedical Press, Amsterdam
27 Knöppel, E., Eisenberg, D. and Wickner, W. (1979) Biochemistry 18, 4177–4181
28 Mollay, C. (1985) in 'The enzymology of post-translational modifications of proteins' (Freedman, R. and Hawkins, M.C., eds.), Vol. 2, Academic Press, London
29 Inouye, M. (1978) Annu. Rev. Biochem. 47, 481–532
30 Engelmann, D.M. and Steitz (1981) Cell 23, 411–422
31 Von Heijne, G. and Blomberg, C. (1979) Eur. J. Biochem. 97, 175–181
32 Prendergast, F.G., Lu, J., Wei, G.J. and Bloomfield, V.A. (1982) Biochemistry 21, 6963–6971
33 Freer, J.H., Birkbeck, T.H. and Bhakoo, M. (1984) Bacterial Protein Toxins 24, 181–189
34 Dufourc, E.J., Faucon, J.-F., Fourche, G., Dufourcq, J., Gulik-Krzywicki, T. and Le Maire, M. (1986) FEBS Lett. 201, 205–209
35 Dufourcq, J., Faucon, J.-F., Fourche, G., Dasseux, J.-L., Le Maire, M. and Gulik-Krzywicki, T. (1986) Biochim. Biophys. Acta 859, 33–48
36 De Kruijff, B., Cullis, P.R., Verkleij, A.J., Hope, M.J., Van Echteld, C.J.A. and Taraschi, T.F. (1985) in The Enzymes

of Biological Membranes (Martinosi, A., ed.), pp. 131–204, Plenum Press, New York
37 Batenburg, A.M., Hibbeln, J.C.L. and De Kruijff, B. (1987) Biochim. Biophys. Acta 903, 155–165
38 Smaal, E.B., Romijn, D., Geurts van Kessel, W.S.M., De Kruijff, B. and De Gier, J. (1985) J. Lipid Res. 26, 633–637
39 Mollay, C., Kreil, G. and Berger, H. (1976) Biochim. Biophys. Acta 426, 317–324
40 Wilschut, J., Düzgünes, N., Fraley, R. and Papahadjopoulos, D. (1980) Biochemistry 19, 6011–6021
41 Szoka, F.C. and Papahadjopoulos, D. (1978) Proc. Natl. Acad. Sci. USA 75, 621–625
42 Fiske, C.M. and SubbaRow, Y. (1925) J. Biol. Chem. 66, 375–389
43 Rouser, G., Fleischer, S. and Yamamoto, A. (1975) Lipids 5, 494–496
44 Hille, J.D.R., Donné-Op den Kelder, G.M., Sauve, P., De Haas, G.H. and Egmond, M.R. (1981) Biochemistry 20, 4068–4073
45 Chupin, V., Killian, J.A. and De Kruijff, B. (1987) Biophys. J. 51, 395–405
46 Sitte, H., Edelmann, L. and Neumann, K. (1987) in Cryotechniques in Biological Electron Microscopy (Steinbrecht, R.A. and Zierold, K., eds.), Springer Verlang, Berlin, in the press
47 Struck, D.K., Hoekstra, D. and Pagano, R.E. (1981) Biochemistry 20, 4093–4099
48 Tilcock, C.P.S., Cullis, P.R. and Gruner, S.M. (1986) Chem. Phys. Lipids 40, 47–59
49 Seelig, J. (1978) Biochim. Biophys. Acta 515, 105–140
50 Batenburg, A.M., Bougis, P.E., Rochat, H., Verkleij, A.J. and De Kruijff, B. (1985) Biochemistry 24, 7101–7110
51 De Kruijff, B. and Cullis, P.R. (1980) Biochim. Biophys. Acta 601, 235–240
52 De Kruijff, B., Verkleij, A.J., Leunissen-Bijvelt, J., Van Echteld, C.J.A., Hille, J. and Rijnbout, H. (1982) Biochim. Biophys. Acta 693, 1–12
53 Verkleij, A.J., Mombers, C., Leunissen-Bijvelt, J. and Ververgaert, P.J.T. (1979) Nature (London) 279, 162–163
54 Hauser, H. (1984) Biochim. Biophys. Acta 772, 37–50
55 De Kruijff, B., Rietveld, A., Telders, N. and Vaandrager, B. (1985) Biochim. Biophys. Acta 820, 295–304
56 Luzzati, V., Tandieu, A., Gulik-Krzywicki, T., Rivas, E. and Reiss-Husson, F. (1968) Nature (London) 220, 485–488
57 Wilschut, J., Holsappel, M. and Jansen, R. (1982) Biochim. Biophys. Acta 690, 297–301
58 Eytan, G.D. and Almary, T. (1983) FEBS Lett. 156, 29–32
59 Verkleij, A.J. (1984) Biochim. Biphys. Acta 779, 43–63
60 Hui, S.W., Stewart, T.P. and Boni, L.T. (1983) Chem. Phys. Lipids 33, 113–126
61 Verkleij, A.J., Mombers, C., Gerritsen, W.J., Leunissen-Bijvelt, J. and Cullis, P.R. (1979) Biochim. Biophys. Acta 555, 358–361
62 Luzzati, V., Gulik, A., Gulik-Krzywicki, T. and Tardieu, A. (1986) in Lipids and Membranes: Past, Present and Future (Op den Kamp, J.A.F., Roelofsen, B. and Wirtz, K.W.A., eds.), pp. 137–151, Elsevier Science Publishers, Amsterdam
63 Rilfors, L., Eriksson, P.-O., Arvidson, G. and Lindblom, G. (1986) Biochemistry 25, 7702–7711
64 Dufourc, E.J., Smith, I.C.P. and Dufourcq, J. (1986) Biochemistry 25, 6448–6455
65 Cullis, P.R., De Kruijff, B., Hope, M.J., Verkleij, A.J., Nayar, R., Farren, S.B., Tilcock, C., Madden, T.D. and Bally, M.B. (1983) in Membrnae Fluidity (Alioa, R.C., ed.), Vol. 2, pp. 40–79, Academic Press, New York
66 Nagaraj, R. (1984) FEBS Lett. 165, 79–82
67 Briggs, M.S., Cornell, D.G., Dluhy, R.A. and Gierasch, L.M. (1986) Science 233, 206–208